Chemical Engineering Research and Design 209 (2024) 81–93

Contents lists available at ScienceDirect

Chemical Engineering Research and Design

journal homepage: www.elsevier.com/locate/cherd

Adaptive state feedback controller design for efficient biodiesel production under kinetic uncertainty

Yu Yang *, Juliette Harper

Department of Chemical Engineering, California State University Long Beach, Long Beach, CA 90840, USA

ARTICLE INFO

Keywords:
Adaptive state feedback control
Model predictive control
Moving horizon estimator
Biodiesel

ABSTRACT

In this study, we optimize the quality and economic performance of biodiesel production through a scenario-based adaptive state feedback control framework. Our goal is to maximize the operational efficiency while ensuring the production of on-spec biodiesel, despite uncertainties in reaction kinetics. A first-principle model is employed to describe the process dynamics, with kinetic parameters estimated online using a moving horizon estimator (MHE). A pool of state feedback controllers is created via off-line nonlinear optimization and metaheuristic algorithm based on sampled kinetic scenarios. Then, the uncertainty space is partitioned into several clusters, each linked to an optimal controller from the pool. During online operation, the appropriate controller is selected by matching the estimated kinetic parameters to the corresponding cluster. Simulation studies on a semi-batch reactor demonstrate that manipulating the methanol feed flow rate and heat duty with our control approach significantly improves operational efficiency, reduces online computational time, and enhances robustness to kinetic uncertainties compared to model predictive control (MPC).

1. Introduction

Fossil fuels are a critical concern in the energy sector, mainly due to their significant greenhouse gas emissions. To mitigate the environmental impact of the fuel industry, biofuels producing from animal fat or vegetable oil have emerged as a viable alternative. For example, it has been shown that biodiesel offers comparable engine performance to conventional fuel while reducing the carbon dioxide significantly (Graboski and McCormick, 1998). To facilitate widespread adoption of biodiesel, producers should minimize the production cost while keeping the product quality on-spec. Biodiesel production, which relies on a semi-batch transesterification process, is influenced by several operating factors, such as the molar ratio between alcohol and triglycerides, reaction time, and reaction temperature, which should be controlled properly (Benavides and Diwekar, 2012a). Additionally, uncertainties like feedstock composition and reaction kinetics can affect production rate, quality, and economics, which should be addressed effectively (Benavides and Diwekar, 2012b). Our research aims to design an effective control strategy to ensure that the process is operated on an optimal condition while robust enough to uncertainties. To this end, we begin by reviewing and discussing the model predictive control (MPC), state feedback controller, moving horizon estimator (MHE), and kinetic uncertainty.

MPC: Conventional MPC focuses on the setpoint tracking, which minimizes the disparity between system outputs and desired setpoint through future dynamics prediction and online optimization. In addition, integrating operational constraints into the control action design is a unique advantage of MPC compared to the traditional PID controllers. In biodiesel production, the setpoint is often the mass content of fatty acid methyl esters (FAME) in the effluent. Brásio et al. (2013) has shown that a nonlinear MPC can effectively drive the process output to reach the standard value of FAME, provided the process model is accurate enough. However, their work did not address three critical issues in the MPC design, including the computational cost, robustness, and economic performance.

- The computational load of MPC is usually high due to its optimization-based nature. This drawback becomes even worse especially for nonlinear systems. A common strategy to mitigate this issue is shifting the online computations to offline, such as explicit MPC (Alessio and Bemporad, 2009).
- An inaccurate model used in MPC may lead to offset or even instability. Hence, various robust MPC design methods, such as invariant set-based (Mayne et al., 2005), tube-based (Limon et al.), scenario-based (Bernardini and Bemporad, 2009), and Lyapunov-based (Mhaskar et al., 2006), have been broadly studied.
- The process industry is more interested in the optimal operations beyond the setpoint tracking (Engell, 2007), which requires advanced controller, such as MPC, to incorporate production profit

* Corresponding author.
E-mail address: yu.yang@csulb.edu (Y. Yang).

https://doi.org/10.1016/j.cherd.2024.07.056
Received 30 June 2024; Received in revised form 26 July 2024; Accepted 26 July 2024
Available online 29 July 2024

or cost into the objective function of the optimization framework, leading to the development of economic MPC (EMPC) (Rawlings et al., 2012; Ellis et al., 2014). However, the EMPC has more complex structure than the traditional MPC, resulting in a higher computational burden. In addition, achieving a balance between control and economic performance needs extensive tuning.

These three challenges, computational cost, robustness, and economic performance, may simultaneously degrade MPC performance and thus deserve a unified solution. For example, (Lucia et al., 2014) studied economic robustness of a polymerization batch process and found that the batch time can be more effectively reduced by multi-stage NMPC using a scenario-tree, compared to open-loop robust MPC and affine control policies. However, that approach only branched the scenario tree in the first stage to save the computational cost. Even though more scenarios and stages in the multi-stage NMPC may enhance the controller robustness, the online computational demand will rise rapidly and render the resulting problem unsolvable.

State Feedback Controller: The state feedback controller employs a pre-determined gain matrix to compute control actions in a closed-loop manner, and thus requires minimal online computations. The classical linear-quadratic regulator (LQR) provides an analytical formula of optimal gain matrix for linear system without considering constraint. The linear matrix inequality (LMI) is a popular optimization tool to determine the gain matrix for linear or switched linear systems subject to uncertainties or constraints (Montagner et al., 2006). However, nonlinear systems are more complex, which may require multiple models and controllers to handle a wide operation regime. A common approach is to linearize the process at different operational points and design a state feedback controller for each sub-domain individually (Wang et al., 2007). So far, most state feedback control approaches focus on the robustness and system nonlinearity, whereas the economic performance is rarely studied.

MHE: The controller robustness can be enhanced through a state or parameter estimator to reduce uncertainties. In many works (Nagy and Braatz, 2003; Huang et al., 2012; Voelker et al., 2013; Jung et al., 2015; Dong and Angeli, 2020), the extended Kalman filter (EKF) or MHE are commonly integrated with feedback controllers for process regulation under uncertainties. MHE solves a constrained optimization problem to estimate process states or parameters by fitting past observations over a pre-defined time horizon (Rao et al., 2001). Several critical studies have demonstrated that MHE generally offers superior estimation performance compared to EKF for chemical reactions albeit with higher computational demands (Haseltine and Rawlings, 2005; Alexander et al., 2023). In batch processes, MHE is applied to handle batch-to-batch parameter drifting (Kwon et al., 2015) and multi-rate measurement (Bae et al., 2021). However, because MHE needs a long observation window to ensure the estimation accuracy (Al-Matouq and Vincent, 2015), its effectiveness for a batch process could be limited when in-situ measurement has significant delay or the batch time should be minimized.

Control under kinetic uncertainty: Kinetic parameters are usually subject to uncertainties in the chemical reaction. A scenario-based approach can be employed to address kinetic uncertainty to form a multi-stage multi-scenario formula (Adloor and Vassiliadis, 2021). However, it needs significantly long time to obtain an optimal solution, and thus cannot be used for real-time control problem. A distributionally robust discrete control problem was studied for microbial fermentation under kinetic uncertainty. It adopts an evolutionary computation algorithm to solve a min–max problem with semi-infinite constraints embedded, but also takes substantially long time (Wang et al., 2023). The multistage and worst-scenario NMPCs were compared in a study of the semi-batch reactor regulation subject to kinetic uncertainty (Kummer et al., 2020). It found that the former is 38 times slower than the latter without remarkable improvement in reactor performance. Nevertheless, the design based on worst-scenario could be very conservative.

The goal of this paper is to optimize the biodiesel production efficiency under kinetic uncertainties using an adaptive state feedback control scheme. We define production efficiency as the ratio of batch production profit to the batch time. This measure poses significant challenge to the conventional MPC as the batch time should be treated as an online optimization variable. In addition, the kinetic uncertainty also renders the online optimization more difficult. Inspired by the adaptive state feedback controller designed based on multiple models (Narendra and Balakrishnan, 1997), we firstly sample the kinetic parameter space to generate several scenario sets for controller design and evaluation. Then, a series of nonlinear optimization problems are solved offline based on each sampled scenario to design gain matrices and tune batch time. The resulting controller performance is assessed by the evaluation set. We further employ the particle swarm optimization (PSO) algorithm to search in the kinetic space and design better controllers. Consequently, a pool of state feedback controller can be created. Next, the uncertainty space is divided into several clusters, each associated with an optimal state feedback controller selected from the pool. During online operations, we apply MHE for kinetic parameters estimation, identify the relevant cluster, and choose the proper state feedback controller. The proposed controller design scheme has the following merits:

- The proposed scenario-based state feedback controller can be optimized and evaluated purely offline to avoid high online computational load.
- The PSO algorithm enables multiple controllers generation through intelligent sampling.
- The MHE combined with kinetic parameter clustering can direct the online state feedback controller gain selection to mitigate kinetic uncertainties.
- Switching among multiple controllers can optimize the batch process efficiency and ensure FAME specification under a wide range of kinetic uncertainties.

We demonstrate the computational, economic, and robust superiority of the proposed control scheme over classical nonlinear MPC integrated with MHE on the testing scenario of biodiesel production process. Because we do not assume the similarity or correlation among different batches, the well-known iterative learning control (Lee and Lee, 2007) is excluded from our investigation.

The rest of this paper is organized as follows. The biodiesel production process model is described in Section 2. The proposed adaptive state feedback controller together with PSO and MHE, are presented in Section 3. The comparisons between classical MPC and state feedback control on the simulated batch reaction are conducted in Section 4 to highlight the superiority of the proposed scheme on economic performance and robustness. Finally, conclusions are drawn in Section 5.

Notation. Throughout this paper, vectors and matrices are denoted by boldface letters. The overline and underline represent the upper and lower bounds on a variable. The operator $|\cdot|$ on a set calculates its cardinality.

2. Biodiesel production process

The transesterification reaction breaks down triglycerides into glycerol and FAME using alcohol, typically methanol or ethanol. This process involves a series of sequential steps: one for each glyceride, tri-, di- and monoglyceride. The reactions are shown below:

$$TG + \mathrm{CH_3OH} \underset{k_2}{\overset{k_1}{\rightleftharpoons}} DG + FAME, \tag{1}$$

$$DG + \mathrm{CH_3OH} \underset{k_4}{\overset{k_3}{\rightleftharpoons}} MG + FAME, \tag{2}$$

$$MG + \mathrm{CH_3OH} \underset{k_6}{\overset{k_5}{\rightleftharpoons}} G + FAME. \tag{3}$$

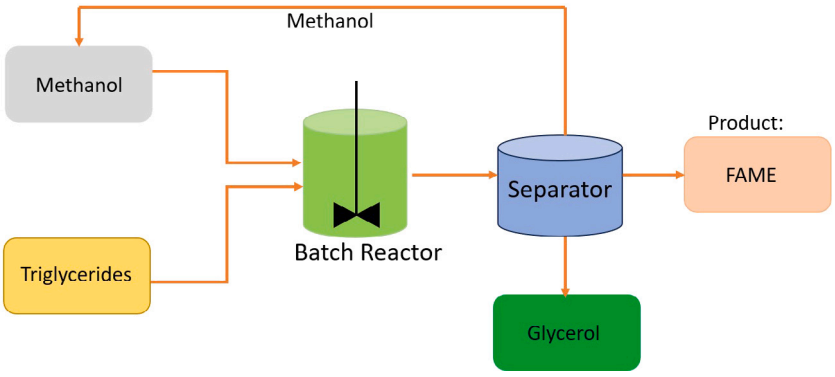

Fig. 1. The biodiesel production scheme.

In Eq. (1), triglycerides, denoted as TG, typically derived from vegetable oils, are reacted with methanol, CH_3OH, to produce diglyceride, denoted as DG, and FAME. Eq. (2) illustrates the subsequent reaction between DG and CH_3OH. Then, the monoglyceride, denoted MG, is formed along with additional FAME. In Eq. (3) of this three-step process, the MG yielded from Eq. (2) is reacted with CH_3OH, to generate glycerol, denoted as G, along with the final FAME. Assuming complete conversion, each mole of triglyceride yields three moles of FAME, making transesterification an efficient method for biodiesel production. In addition to the batch reactor, a separator is needed to split the crude biodiesel from the remaining components in batch reactors. Unreacted methanol can be recycled into the reactor for subsequent batches. An overview of the production system is shown in Fig. 1.

We use the following mass and energy balance equations to describe the transesterification reaction (Brásio et al., 2013).

$$m\frac{dx_i}{dt} = F(x_{0,i} - x_i) + \phi_i,\ i = 1, 2, \dots, 6, \tag{4}$$

$$\rho A\frac{dh}{dt} = F + V\rho^2 \sum_{i=1}^{6} \frac{1}{\rho_i}\frac{dx_i}{dt}, \tag{5}$$

$$\rho C_p V\frac{dT}{dt} = FC_{p,F}(T_F - T) + \sum_{j=1}^{3}(\Delta H)_j r_j V + Q_w, \tag{6}$$

where x_i is the component mass fraction; m is the total mass in the reactor with unit gram; h is the reactor liquid level with unit dm; A is the cross-sectional area of the reactor with unit dm^2; V is the volume of mixture with unit liter; T is the reaction temperature in Kelvin; Q_w is the heat duty; T_F, $C_{p,F}$, and F are the temperature, heat capacity, and the mass flow rate of feeding methanol, respectively; $(\Delta H)_j$ is the heat of reaction; the mixture density ρ and specific heat capacity C_p are dependent on each component density ρ_i and heat capacity $C_{p,i}$:

$$\rho = \left(\sum_{i=1}^{6}\frac{x_i}{\rho_i}\right)^{-1},\ C_p = \sum_{i=1}^{6} C_{p,i}x_i. \tag{7}$$

The reaction rate r_j is defined as follows:

$$r_1 = k_1C_2C_1 - k_2C_3C_6, \tag{8}$$

$$r_2 = k_3C_3C_1 - k_4C_4C_6, \tag{9}$$

$$r_3 = k_5C_4C_1 - k_6C_5C_6, \tag{10}$$

where $C_{p,i}, i = 1, 2, 3 \dots, 6$ is the mole concentration of components 1 to 6. Here the reaction rate $\boldsymbol{k} = [k_1, k_2, \dots, k_6]^{\mathrm{T}}$ shown in Eqs. (1)–(3) is specified by the Arrhenius equation,

$$k_b = k_{0,b}\exp\left(\frac{-E_b}{RT}\right),\ b = 1, 2, \dots, 6, \tag{11}$$

where $\boldsymbol{k}_0 = [k_{0,1}, k_{0,2}, \dots, k_{0,6}]^{\mathrm{T}}$ is the pre-exponential factor; E_b is the energy of activation; R is the ideal gas constant. The generation reaction terms are shown below:

$$\phi_1 = -(r_1 + r_2 + r_3)VM_1,\ \phi_2 = -r_1VM_2, \tag{12}$$

Table 1
Component parameters.

i	1	2	3	4	5	6
Name	CH_3OH	TG	DG	MG	FAME	G
ρ_i (g/L)	769	914.37	941.90	990.56	856.37	1346.60
M_i	32.04	873.06	612.74	352.42	292.36	92.09
$C_{p,i}$ (J/gK)	2.705	2.052	2.119	2.284	2.084	2.509

Table 2
Nominal kinetic parameters.

b	1	2	3	4	5	6
E_b	16 377	19 202	17 867	19 383	15 302	4282
$\tilde{k}_{0,b}$	0.5401	1.1180	4.3119	3.7486	0.0397	0.0317

$$\phi_3 = (r_1 - r_2)VM_3,\ \phi_4 = (r_2 - r_3)VM_4, \tag{13}$$

$$\phi_5 = r_3VM_5,\ \phi_6 = (r_1 + r_2 + r_3)VM_6, \tag{14}$$

where $M_i,\ i = 1, 2, \dots, 6$ is the molar weight of each component. The values of parameters are shown in Tables 1 and 2.

The nominal value of the pre-exponential factor, denoted as $\tilde{k}_{0,b}$, is derived from experimental data at $T = 323$ K Berchmans et al. (2010). However, actual reaction kinetics may vary between batches. Thus, we introduce uncertainties on $\boldsymbol{k}_0$ with ±30% of their nominal values in the simulation. A larger variance of $\boldsymbol{k}_0$ will render the control task more challenging. However, because we use a sampling-based method to evaluate the impact of kinetic uncertainty on the developed controllers, the proposed method is more robust and less conservative than the conventional or worst-case MPC. We expect that this advantage becomes more remarkable under larger variance of $\boldsymbol{k}_0$.

The quality specification of biodiesel requires the FAME percentage χ_E to be greater than 98.8% by following the standard EN 14214:2008 (Brásio et al., 2013).

$$\chi_E = \frac{x_5}{x_2 + x_3 + x_4 + x_5} \geqslant 98.8\% \tag{15}$$

The profit of biodiesel production $(x_2 + x_3 + x_4 + x_5)$ is calculated based on the biodiesel sales P_d = \$1.19 per liter, methanol cost P_m = \$526 per metric ton, electricity price P_e = \$0.0832 per kWh, energy consumption for separation of methanol E_s = 0.374 kWh/kg, and soybean oil cost per batch P_s = \$725.05.

$$\begin{aligned}\text{Profit} = {} & P_d \cdot \text{Biodiesel Production} - P_m \cdot (\text{Consumed Methanol} \\ & + 10\%\text{Unreacted Methanol}) \\ & - P_s - P_e \cdot (\text{Heating Energy} + E_s \cdot 90\%\text{Unreacted Methanol})\end{aligned} \tag{16}$$

Here we assume that 90% of unreacted methanol in a batch can be recycled. However, separation of such amount of methanol from the batch effluent needs to consume some extra energy.

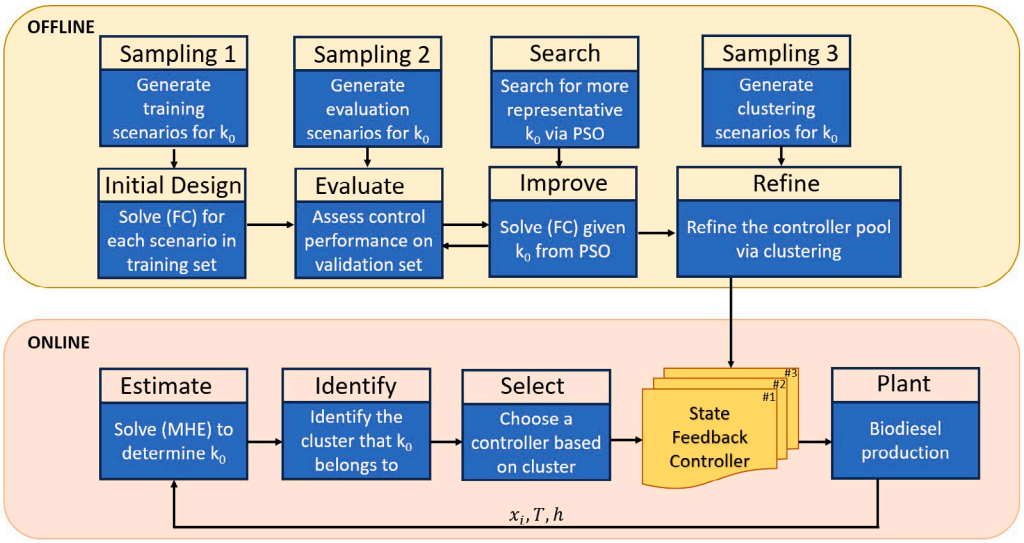

Fig. 2. The overall controller design and application scheme.

3. Control system design

The purpose of control is to maximize the biodiesel production process efficiency while ensuring the product quality specification. The proposed control system design involves two phases. In the offline design phase, we sample the uncertain parameter $\boldsymbol{k}_0$ to generate a training set, denoted as Γ, an evaluation scenario set, denoted as Π, and a clustering scenario set, denoted as Φ, respectively. The state feedback controllers are initially designed based on each scenario of $\boldsymbol{k}_0$ in the training set Γ. Then, the scenarios in evaluation set are used to determine the average process efficiency using the proposed controllers. A PSO-based scheme is developed to further improve these controllers by searching for more representative kinetic parameter values and solving the associated optimal control problem. During this searching process, a pool of controllers is created. Finally, the uncertainty space is divided into several clusters using the larger and more representative set Φ. Each cluster is equipped with the best controller from the pool. In the online implementation phase, the MHE is solved at each time instant to estimate kinetic parameter $\boldsymbol{k}_0$ and identify the cluster that it belongs to. Subsequently, the state feedback controller associated with that cluster can be chosen to regulate the plant. This design and application scheme is shown in Fig. 2.

3.1. State feedback control design and evaluation

In this section, we describe the concept of state feedback control based on a sampled kinetic parameter vector. First, let us introduce the optimization-based state feedback controller design formula. The biodiesel production process has two inputs F and Q_w. Their state feedback control law is shown in (17) and (18):

$$\begin{bmatrix} F \\ Q_w \end{bmatrix} = \begin{bmatrix} \boldsymbol{K}_F \\ \boldsymbol{K}_Q \end{bmatrix} \begin{bmatrix} \boldsymbol{x} \\ h \\ T \end{bmatrix} + \begin{bmatrix} Y_F \\ Y_Q \end{bmatrix}, \tag{17}$$

$$F \leftarrow \min\{\overline{F}, F\},\ F \leftarrow \max\{\underline{F}, F\},\ Q_w \leftarrow \min\{\overline{Q}_w, Q_w\},\ Q_w \leftarrow \max\{\underline{Q}_w, Q_w\}, \tag{18}$$

where $\boldsymbol{x} = [x_1, x_2, \dots, x_6]^{\mathrm{T}}$; $\boldsymbol{K}_F \in \mathbb{R}^{1\times 8}$ and $\boldsymbol{K}_Q \in \mathbb{R}^{1\times 8}$ are feedback gain; $Y_F \in \mathbb{R}$ and $Y_Q \in \mathbb{R}$ are constants. Eq. (18) enforces the control inputs to be within the lower and upper bounds on F and Q_w. The offline design task is to determine $\{\boldsymbol{K}_F, \boldsymbol{K}_Q, Y_F, Y_Q\}$.

Given the kinetic parameter $\boldsymbol{k}_0$, we develop a model-based prediction scheme to optimize the production efficiency and determine controller parameters offline:

$$\begin{aligned} \mathcal{E}(\boldsymbol{k}_0) = \min_{\boldsymbol{K}_F, \boldsymbol{K}_Q, Y_F, Y_Q} \frac{1}{D_p} \Big(& P_d m(D_p) \big(x_2(D_p) + x_3(D_p) \\ & + x_4(D_p) + x_5(D_p) \big) - P_s \\ & - P_m \Big(\sum_{l=1}^{D_p} F(l) + 0.1 m(D_p) x_1(D_p) \Big) \\ & - P_e \Big(\sum_{l=1}^{D_p} Q_w(l)\delta + 0.9 E_s \cdot m(D_p) x_1(D_p) \Big) \Big) \end{aligned} \tag{$\mathcal{FC}$}$$

$$\text{s.t. } m\big(x_i(l) - x_i(l-1)\big) = \delta F(l-1)\big(x_{0,i} - x_i(l-1)\big) + \delta\phi_i,\ i = 1, 2, \dots, 6, \tag{19}$$

$$\rho A\big(h(l) - h(l-1)\big) = \delta F(l-1) + \delta V \rho^2 \sum_{i=1}^{6} \frac{1}{\rho_i} \left(\frac{x_i(l) - x_i(l-1)}{\delta} \right) \tag{20}$$

$$\begin{aligned} \rho C_p V \big(T(l) - T(l-1)\big) = {} & \delta C_{p,F}(T_F - T(l-1)) \\ & + \delta \sum_{j=1}^{3} (\Delta H)_j r_j V + \delta Q_w(l-1), \end{aligned} \tag{21}$$

$$\text{Eqs. (7)–(14), (17), } \forall l \in \{1, 2, \dots, D_p\},$$

$$\chi_E(l) \geqslant 98.8\%,\ \forall l \in \{D_c + 1, D_c + 2, \dots, D_p\}, \tag{22}$$

$$F(l) = 0,\ \forall l \in \{D_c + 1, D_c + 2, \dots, D_p\}, \tag{23}$$

$$F(l) \in [\overline{F}, \underline{F}],\ \forall l \in \{1, 2, \dots, D_c\},\ Q_w(l) \in [\overline{Q}_w, \underline{Q}_w],$$
$$\forall l \in \{1, 2, \dots, D_p\}, \tag{24}$$

where D_c is the control horizon and D_p is the prediction horizon. Eqs. (19)–(21) are derived through the finite difference method to discrete the process model (4)–(6) with the sampling time interval as $\delta = 30$ s. Eq. (22) enforces χ_E to reach the desired quality 98.8% by the end of control horizon. After D_c time instants, the input methanol can be set as $F = 0$ and it usually takes around 6.5 min to reach the steady state. In our simulation, we thus set $D_p = D_c + 13$. The objective function of ($\mathcal{FC}$) is the production profit per unit time instant. For the transesterification reaction, the time to reach desired 98.8% FAME can be shortened if the methanol input is maximized. However, excessive methanol in the reactor may increase the recycle duty and unnecessary depletion. Hence, the efficiency (profit per unit time instant) is a more suitable index to characterize the production performance compared to

the batch time or total profit. The associated challenge is that the optimal D_p varies given different $\boldsymbol{k}_0$ value and depends on the employed controller. Thus, we may need to enumerate D_p in a specific range and solve resulting ($\mathcal{FC}$) individually. This manner may prolong the offline computational time but enhance the optimality on the prediction horizon. Here we employ the IPOPT (Wächter and Biegler, 2006) to solve ($\mathcal{FC}$) and let $\{\boldsymbol{K}_F^{k_0}, \boldsymbol{K}_Q^{k_0}, Y_F^{k_0}, Y_Q^{k_0}\}$ to denote the solution given the kinetic model parameter $\boldsymbol{k}_0$.

Note that the proposed controller in ($\mathcal{FC}$) is designed only based on the specific $\boldsymbol{k}_0$, which is subject to uncertainty in practical operations. It is thus necessary to evaluate the controller performance under model mismatch. To this end, we calculate the average process efficiency across all scenarios in the evaluation set Π. Let $\mathcal{E}(\boldsymbol{k}_0'; \boldsymbol{k}_0)$ denote the process efficiency with actual kinetic parameter $\boldsymbol{k}_0' \in \Pi$, but regulated by the controller derived in ($\mathcal{FC}$) based on parameter $\boldsymbol{k}_0 \in \Gamma$. We can simulate the process model in Eqs. (7)–(14) to obtain the process efficiency.

$$\begin{aligned}\mathcal{E}(\boldsymbol{k}_0'; \boldsymbol{k}_0) = \frac{1}{D_p}\Bigg(& P_d m(D_p, \boldsymbol{k}_0'; \boldsymbol{k}_0)\big(x_2(D_p, \boldsymbol{k}_0'; \boldsymbol{k}_0) + x_3(D_p, \boldsymbol{k}_0'; \boldsymbol{k}_0) \\ & + x_4(D_p, \boldsymbol{k}_0'; \boldsymbol{k}_0) + x_5(D_p, \boldsymbol{k}_0'; \boldsymbol{k}_0)\big) \\ & - P_s - P_m\Big(\sum_{l=1}^{D_p} F(l, \boldsymbol{k}_0'; \boldsymbol{k}_0) + 0.1 m(D_p, \boldsymbol{k}_0'; \boldsymbol{k}_0) x_1(D_p, \boldsymbol{k}_0'; \boldsymbol{k}_0)\Big) \\ & - P_e\Big(\sum_{l=1}^{D_p} Q_w(l, \boldsymbol{k}_0'; \boldsymbol{k}_0)\delta + 0.9 E_s \cdot m(D_p, \boldsymbol{k}_0'; \boldsymbol{k}_0) x_1(D_p, \boldsymbol{k}_0'; \boldsymbol{k}_0)\Big)\Bigg)\end{aligned} \tag{25}$$

where $m(D_p, \boldsymbol{k}_0'; \boldsymbol{k}_0)$, $x_i(D_p, \boldsymbol{k}_0'; \boldsymbol{k}_0), \forall i = 1, 2, \ldots, 5$, and $F(l, \boldsymbol{k}_0'; \boldsymbol{k}_0)$ are process variables with model parameter $\boldsymbol{k}_0'$ and controller parameters $\{\boldsymbol{K}_F^{k_0}, \boldsymbol{K}_Q^{k_0}, Y_F^{k_0}, Y_Q^{k_0}\}$. Here D_p is based on our previous setting: $D_p = D_c + 13$ and D_c is determined when χ_E reaches the desired values 98.8%. Then, the average performance of a controller derived from a specific $\boldsymbol{k}_0$ is:

$$\tilde{\mathcal{E}}(\boldsymbol{k}_0) = \frac{\sum_{\boldsymbol{k}_0' \in \Pi} \mathcal{E}(\boldsymbol{k}_0'; \boldsymbol{k}_0)}{|\Pi|} \tag{26}$$

3.2. Controller improvement and refinement

Controller Improvement: In this subsection, we discuss how to improve the controller performance characterized by simulation over multiple scenarios shown in Eq. (26). One may consider to form a large-scale optimization formula for $\{\boldsymbol{K}_F, \boldsymbol{K}_Q, Y_F, Y_Q\}$ across all sampled scenarios simultaneously. However, three issues should be addressed:

1. The prediction horizon D_p varies across scenarios and is hard to be pre-determined.
2. The resulting large-scale multi-scenario multi-step prediction model is highly nonlinear, making it challenging to secure a high-quality solution.
3. If we can estimate $\boldsymbol{k}_0$ through MHE, then an adaptive control scheme might be more suitable than a single controller optimized for all kinetic scenarios.

Therefore, we employ an intelligent optimization approach, PSO, to generate additional $\boldsymbol{k}_0$ samples, solve resulting ($\mathcal{FC}$) sequentially, and build a controller pool. Note that PSO is a well-established methodology with numerous variations. The aim of this paper is not to create a new PSO method, but to utilize the classical adaptive PSO scheme (Zhan et al., 2009). The essential steps and modifications are outlined in Algorithm 1. Totally $|\Gamma|$ particles are considered in this scheme. Each particle represents a search agent for the kinetic parameter $\boldsymbol{k}_0$.

In Algorithm 1, the training set Γ consists of all the initial scenarios $\boldsymbol{k}_0^{0,m}$ and Γ' is an enlarged set storing all sampled kinetic scenarios. Index g denotes the evolving iteration and index m denotes the particle. **Vec** is the velocity vector of particles. ω^g is the inertia weight. c_1^g and c_2^g are the acceleration coefficients. $\boldsymbol{\alpha}_1^{g,m}$ and $\boldsymbol{\alpha}_2^{g,m}$ are two uniformly distributed random vectors independently generated within $[0, 1]$. The particle's new position $\boldsymbol{k}_0^{g,m}$ is calculated by adding the velocity vector to the previous position and restricted by the searching range $[\underline{\boldsymbol{k}}_0, \overline{\boldsymbol{k}}_0]$. The controller average performance $\tilde{\mathcal{E}}$ is used as the fitness function in PSO; $\mathbf{pBest}^m$ is the kinetic vector corresponding to the best controller found by mth particle. **gBest** is the kinetic vector corresponding to the best controller among all particles. The updating formula of evolution factor, parameters ω, c_1 and c_2 can be found in Ref. Zhan et al. (2009). The number of evolving iteration is denoted as G. The number of particles is initialized as $|\Gamma|$, which implies that we solve $|\Gamma|$ scenarios and generate the same number of controllers at each iteration. Consequently, there should be $|\Gamma'| = G|\Gamma|$ controllers in the pool. Different from conventional PSO that only keeps the optimal solution **gBest**. Here we collect all investigated $|\Gamma'|$ controllers and associated $\tilde{\mathcal{E}}$ for next step: controller refinement.

output: $\boldsymbol{K}_F^{k_0^{g,m}}, \boldsymbol{K}_Q^{k_0^{g,m}}, Y_F^{k_0^{g,m}}, Y_Q^{k_0^{g,m}}, \forall \boldsymbol{k}_0^{g,m} \in \Gamma'$

Initialize: Γ, $c_1^{1,m}$, $c_2^{1,m}$, ω^1, $\boldsymbol{k}_0^{0,m}$;
for $g \leftarrow 1$ **to** G **do**
  for $m \leftarrow 1$ **to** $|\Gamma|$ **do**
    $\mathbf{Vec}^{g,m} = \omega^g \mathbf{Vec}^{g-1,m} + c_1^g \boldsymbol{\alpha}_1^{g,m}(\mathbf{pBest}^m - \boldsymbol{k}_0^{g-1,m}) + c_2^g \boldsymbol{\alpha}_2^{g,m}(\mathbf{gBest} - \boldsymbol{k}_0^{g-1,m})$;
    $\boldsymbol{k}_0^{g,m} \leftarrow \boldsymbol{k}_0^{g-1,m} + \mathbf{Vec}^{g,m}$;
    $\boldsymbol{k}_0^{g,m} \leftarrow \max\{\boldsymbol{k}_0^{g,m}, \underline{\boldsymbol{k}}_0\}$; $\boldsymbol{k}_0^{g,m} \leftarrow \min\{\boldsymbol{k}_0^{g,m}, \overline{\boldsymbol{k}}_0\}$;
    Solve ($\mathcal{FC}$) with $\boldsymbol{k}_0^{g,m}$ and $D_p \in [\underline{D}_p, \overline{D}_p]$ to obtain $\mathcal{E}(\boldsymbol{k}_0^{g,m})$ and $\boldsymbol{K}_F^{k_0^{g,m}}, \boldsymbol{K}_Q^{k_0^{g,m}}, Y_F^{k_0^{g,m}}, Y_Q^{k_0^{g,m}}$;
    Calculate $\tilde{\mathcal{E}}(\boldsymbol{k}_0^n; \boldsymbol{k}_0^{g,m})$ over the evaluation set $\forall \boldsymbol{k}_0^n \in \Pi$;
    if $\tilde{\mathcal{E}}(\boldsymbol{k}_0^{g,m}) > \tilde{\mathcal{E}}(\boldsymbol{pBest}^m)$ **then**
      Update $\mathbf{pBest}^m$;
    end
  end
  $\Gamma' = \Gamma' \cup \{\boldsymbol{k}_0^{g,m}, \ \forall m = 1, 2, \ldots, |\Gamma|\}$;
  Calculate evolution factor to determine ω^{g+1}, c_1^{g+1}, and c_2^{g+1};
  if $\exists m \in \{1, 2, \ldots, |\Gamma|\}$, $\tilde{\mathcal{E}}(\boldsymbol{k}_0^{g,m}) > \tilde{\mathcal{E}}(\boldsymbol{gBest})$ **then**
    Update **gBest** ;
  end
end

Algorithm 1: PSO for controller improvement

In the PSO framework, we solve ($\mathcal{FC}$) by enumerating D_p to achieve the optimal efficiency and associated batch time for a given $\boldsymbol{k}_0$. However, this exhaustive search could be very time demanding and thus limiting the number of PSO iterations. To resolve this issue, we can develop a regression model to narrow the searching range of D_p given a sampled kinetic parameter $\boldsymbol{k}_0$:

$$\hat{D}_p = \mathcal{D}(\boldsymbol{k}_0), \ D_p \in [\lfloor \hat{D}_p \rfloor, \lceil \hat{D}_p \rceil] \tag{27}$$

where the regression function $\mathcal{D}$ is learned from the existing samples $\boldsymbol{k}_0$ and associated optimal D_p. The range of D_p is rounded down and up to the nearest integers of $\hat{D}_p$.

Controller refinement: Although PSO yields a bunch of controllers, only a few of them will be employed, including the best controller in the pool:

$$\{\boldsymbol{K}_F^{k_0^*}, \boldsymbol{K}_Q^{k_0^*}, Y_F^{k_0^*}, Y_Q^{k_0^*}\} = \arg\max_{\boldsymbol{k}_0 \in \Gamma'} \tilde{\mathcal{E}}(\boldsymbol{k}_0) \tag{28}$$

To develop an adaptive control scheme, we generate a much larger kinetic scenario set Φ and partition it into several groups. The vector components $k_{0,b}$ are normalized based on their nominal values and then fed into the k-means method for clustering. Each cluster is equipped

with a state feedback controller denote as $\{\boldsymbol{K}_{F,j}, \boldsymbol{K}_{Q,j}, Y_{F,j}, Y_{Q,j}\}, \forall j = 1, 2, \ldots, N$. Let $\boldsymbol{\Phi}_1, \boldsymbol{\Phi}_2, \ldots, \boldsymbol{\Phi}_N$ to represent totally N clusters of scenarios, and their centers are $\boldsymbol{\mu}_1, \boldsymbol{\mu}_2, \ldots, \boldsymbol{\mu}_N$, respectively. We choose the state feedback controller from the pool Γ' for jth cluster based on (29):

$$\tilde{\mathcal{E}}^*_{\boldsymbol{\Phi}_j} = \max_{g,m} \frac{\sum_{\forall \boldsymbol{k}_0 \in \boldsymbol{\Phi}_j} \mathcal{E}(\boldsymbol{k}_0; \boldsymbol{k}_0^{g,m})}{|\boldsymbol{\Phi}_j|}, \quad \{g^*, m^*\} = \arg\max_{g,m} \frac{\sum_{\forall \boldsymbol{k}_0 \in \boldsymbol{\Phi}_j} \mathcal{E}(\boldsymbol{k}_0; \boldsymbol{k}_0^{g,m})}{|\boldsymbol{\Phi}_j|} \tag{29}$$

where $\tilde{\mathcal{E}}^*_{\boldsymbol{\Phi}_j}$ is the average efficiency in cluster $\boldsymbol{\Phi}_j$ using the optimal controller from the pool. Then, there is $\{\boldsymbol{K}_{F,j}, \boldsymbol{K}_{Q,j}, Y_{F,j}, Y_{Q,j}\} = \{\boldsymbol{K}_F^{\boldsymbol{k}_0^{g^*,m^*}}, \boldsymbol{K}_Q^{\boldsymbol{k}_0^{g^*,m^*}}, Y_F^{\boldsymbol{k}_0^{g^*,m^*}}, Y_Q^{\boldsymbol{k}_0^{g^*,m^*}}\}$.

3.3. Online control implementation

Because the offline designed controllers are associated with the kinetic clusters, the online control scheme should firstly estimate $\boldsymbol{k}_0$ via MHE, given the measurement of component mass fraction $x_i, i = 1, 2, \ldots, 6$, liquid level h, and reactor temperature T. Let s to denote the current time step index. MHE can be constructed as an optimization formula over a backward window with length D_m: $s - D_m + 1, s - D_m + 2, \ldots, s$.

$$\begin{aligned} \min_{\hat{\boldsymbol{k}}_0} \sum_{l=s-D_m+1}^{s} \sum_{i=1}^{6} & W_i(x_i(l) - \hat{x}_i(l|s))^2 + W_h(h(l) - \hat{h}(l|s))^2 \\ & + W_T(T(l) - \hat{T}(l|s))^2 \\ & + \boldsymbol{W}_{\boldsymbol{a}}^{\mathrm{T}}(\hat{\boldsymbol{k}}_0(s) - \hat{\boldsymbol{k}}_0(s-1)) \end{aligned} \tag{$\mathcal{MHE}$}$$

$$\text{s.t. } m\big(\hat{x}_i(l|s) - \hat{x}_i(l-1|s)\big) = \delta F(l-1)\big(x_{0,i} - \hat{x}_i(l-1|s)\big) + \delta\phi_i(l-1), \quad i = 1, 2, \ldots, 6, \tag{30}$$

$$\rho A\big(\hat{h}(l|s) - \hat{h}(l-1|s)\big) = \delta F(l-1) + \delta V \rho^2 \sum_{i=1}^{6} \frac{1}{\rho_i}\left(\frac{\hat{x}_i(l|s) - \hat{x}_i(l-1|s)}{\delta}\right), \tag{31}$$

$$\begin{aligned} \rho C_p V\big(\hat{T}(l|s) - \hat{T}(l-1|s)\big) = {} & \delta C_{p,F}(T_F - \hat{T}(l-1|s)) \\ & + \delta \sum_{j=1}^{3} (\Delta H)_j r_j V + \delta Q_w(l-1), \end{aligned} \tag{32}$$

$$\text{Eqs. (7)–(14)}, \ l \in \{s - D_m + 1, s - D_m + 2, \ldots, s\},$$

$$\hat{\boldsymbol{k}}_0 \in [0.7\tilde{\boldsymbol{k}}_0, 1.3\tilde{\boldsymbol{k}}_0], \ \hat{x}_i \in [0, 1], \ \hat{T} \in [\underline{T}, \overline{T}], \ \hat{h} \in [\underline{h}, \overline{h}],$$

where W_h, W_T, and $W_i, \forall i = 1, 2, \ldots, 6$, are weighting parameters of the stage cost for each state variable; $\boldsymbol{W}_{\boldsymbol{a}}$ is the weighting parameter of the arrival cost; $\hat{x}_i(l|s)$, $\hat{h}(l|s)$ and $\hat{T}(l|s)$ are estimated state values for time instant l at current time instant s; $\hat{\boldsymbol{k}}_0(s)$ is the estimated parameter value at time instant s.

Several comments on MHE are presented in order. First, the objective function of ($\mathcal{MHE}$) is composed of the sum of stage-wise estimation error over the window and an arrival cost $\boldsymbol{W}_{\boldsymbol{a}}^{\mathrm{T}}(\hat{\boldsymbol{k}}_0(s) - \hat{\boldsymbol{k}}'_0(s-1))$. The weighting parameters within the objective function can be tuned according to the covariance information of each deviation term. The arrival cost helps smooth the estimation of $\boldsymbol{k}_0$ across consecutive time instants. Second, MHE is superior than other estimation approaches because it can integrate various physical bounds directly into the formula. Therefore, we specify upper and lower limits for each estimation variable to improve the estimation accuracy. However, ($\mathcal{MHE}$) is a nonlinear program (NLP) that can only guarantee suboptimal solutions. This inherent characteristic should be considered when evaluating the performance of MHE. Third, the length of the estimation window D_m may impact the estimation performance. A larger D_m allows for the inclusion of more historical data in ($\mathcal{MHE}$), potentially leading to more reliable estimations. However, a longer window increases the online computational demand. More importantly, this semi-batch process has relatively short reaction time. Long data collection period may delay the application of $\hat{\boldsymbol{k}}_0$ in the control scheme. We thus set $D_m = 8$ in the simulation.

Note that MHE needs gathering D_m data to estimate $\boldsymbol{k}_0$. Hence, in the beginning of a batch, we have to employ the best available controller in the pool: $\{\boldsymbol{K}_F^{\boldsymbol{k}_0^*}, \boldsymbol{K}_Q^{\boldsymbol{k}_0^*}, Y_F^{\boldsymbol{k}_0^*}, Y_Q^{\boldsymbol{k}_0^*}\}$. Once enough data points are collected and $\hat{\boldsymbol{k}}_0$ is estimated by MHE, we can identify the cluster that belongs to. The k-means method determines the cluster based on Euclidean distance:

$$j^* = \arg\min_{j \in \{1,2,\ldots,N\}} \|\hat{\boldsymbol{k}}_0 - \boldsymbol{\mu}_j\| \tag{33}$$

Note that $\hat{\boldsymbol{k}}_0$ should be normalized based on their nominal value and then compared with $\boldsymbol{\mu}_j$. Then, the controller can be switched to $\{\boldsymbol{K}_{F,j^*}, \boldsymbol{K}_{Q,j^*}, Y_{F,j^*}, Y_{Q,j^*}\}$, and we use (17) and (18) to determine F and Q_w.

Table 3
Operational constraints.

	Upper bound	Lower bound
F	800 g/s	0 g/s
Q_w	36 kW	−20 kW
T	340 K	290 K
h	30 dm	0 dm

4. Simulation study

In this section, we simulate the biodiesel production process described in Section 2. The hardware platform is a workstation with Intel Xeon Silver 4208 processor and 16 GB memory. The software platform is MATLAB and OPTI toolbox with NLP solver IPOPT.

The simulated batch reactor has a diameter of 1 meter and a height of 3 m. The operational constraints of the biodiesel production process are listed in Table 3. The scenarios are generated as follows. First, the basic variations are chosen randomly from the range [−30%, 30%] of the nominal $\boldsymbol{k}_0$ values shown in Table 2. Additional ±2% time-varying fluctuations are further added to make the simulation more realistic. Here we do not introduce parameter drifting during each batch. An example of the sampled kinetic scenario will be shown in Figs. 5 and 6, Section 4.4.

4.1. Benchmark: Model predictive control

For comparative analysis, we implemented the MPC as an alternative way to control the production process. The MPC is formulated as an online optimization problem with kinetic parameter estimated through ($\mathcal{MHE}$). At each time step s, the MPC formulation involves solving the following problem to determine methanol flow rate F and heat duty Q_w:

$$\min_{F, Q_w} \sum_{l=s+1}^{s+D'_c} (100\chi_E(l|s) - 98.8)^2 + W_{u1}F(l|s)^2 + W_{u2}Q_w(l|s)^2 \tag{$\mathcal{MPC}$}$$

$$\text{s.t. } m\big(\hat{x}_i(l|s) - \hat{x}_i(l-1|s)\big) = \delta F(l-1|s)\big(x_{0,i} - \hat{x}_i(l-1|s)\big) + \delta\phi_i(l-1|s), \ i = 1, 2, \ldots, 6, \tag{34}$$

$$\rho A\big(\hat{h}(l|s) - \hat{h}(l-1|s)\big) = \delta F(l-1|s) + \delta V \rho^2 \sum_{i=1}^{6} \frac{1}{\rho_i}\left(\frac{\hat{x}_i(l|s) - \hat{x}_i(l-1|s)}{\delta}\right), \tag{35}$$

$$\rho C_p V\big(\hat{T}(l|s) - \hat{T}(l-1|s)\big) = \delta C_{p,F}(T_F - \hat{T}(l-1|s)) + \delta \sum_{j=1}^{3} (\Delta H)_j r_j V + \delta Q_w(l-1|s), \tag{36}$$

$$\text{Eqs. (7)–(14)}, \ l \in \{s+1, s+2, \ldots, s+D'_c\},$$

Table 4
Training set: basic variations. Note: Additional ±2% random variations is further introduced.

	$k_{0,1}$	$k_{0,2}$	$k_{0,3}$	$k_{0,4}$	$k_{0,5}$	$k_{0,6}$
Scenario 1	−30%	−30%	−30%	−30%	−30%	−30%
Scenario 2	−25%	−25%	−25%	−25%	−25%	−25%
Scenario 3	0%	0%	0%	0%	0%	0%
Scenario 4	15%	25%	10%	25%	20%	30%
Scenario 5	30%	30%	30%	30%	30%	30%
Scenario 6	−30%	−25%	−20%	−25%	−30%	−25%

Table 5
The performance of each controller derived from 6 training scenarios.

	Optimal D_p	Efficiency in each training scenario	Average efficiency in evaluation set
Controller 1	44	4.6704	5.2226
Controller 2	41	4.8073	5.1876
Controller 3	38	5.4383	5.1959
Controller 4	36	5.7413	5.1897
Controller 5	36	5.9336	5.0740
Controller 6	43	4.6767	5.2295

$$x_i(l|s) \in [0,1],\ T(l|s) \in [\underline{T}, \overline{T}],\ \ h(l|s) \in [\underline{h}, \overline{h}],$$

where $D_c' = 20$ is the control horizon of MPC in this study; Our investigation shows that further increasing D_c' value does not improve the economic performerence of this reactor but significantly extends the computational time; notation $(l|s)$ denotes the prediction of time step l at current time s. Similar with the proposed approach, when χ_E reaches the desired value 98.8%, the methanol flow derived from MPC is overridden to $F = 0$. Subsequently, the operations continue for 6.5 min and then collect the product. Note that formula $(\mathcal{MPC})$ is highly nonlinear due to the complex process model. It is designed for setpoint tracking while the input cost is minimized. According to Ref. Brásio et al. (2013), adjusting the weighting parameter W_{u1} and W_{u2} may improve the process economic efficiency. As the electricity price is significantly less than the methanol cost, we always set $W_{u2} = 0$ to enable high power heating. In addition, we will also tune W_{u1} to investigate its influence on the economic performance of the process. Since kinetic parameters are not known in advance, we use their nominal values in MPC during $1, 2, \ldots, D_m$ time instants. After collecting D_m data points, the MHE provides estimates for the kinetic parameters, which are then incorporated into the MPC for more accurate control.

4.2. State feedback controller design: Initial results

We start by building the training set Γ, which includes 6 kinetic scenarios. The basic variations of these scenarios compared to the nominal one are summarized in Table 4. Here the training set contains the nominal scenario (0%), as well as the slowest (−30%) and fastest (30%) kinetic scenarios to ensure a representative coverage. For each scenario in the training set, we enumerate the prediction horizon $D_p \in [36, 45]$ and solve associated control problem $(\mathcal{FC})$ to determine an optimal state feedback controller. We initially start with a narrow range for the prediction horizon D_p and continuously extend it if the optimal horizon length D_p is found on the boundary of current range. This process is terminated when the optimal D_p value is found within the interior of the range for all scenarios on Table 4, or D_p value results in infeasible problem. In fact, when D_p is set as 35, all scenarios become infeasible because the required reaction time is too short to achieve the desired FAME value. Next, we further sample the kinetic parameter space to generate 113 samples, including 100 fully random scenarios and 13 systematically varied scenarios from −30% to 30% in 5% interval, as an evaluate set for controller performance. The evaluation results of each controller are detailed in Table 5. Here we can observe high variance in efficiency for different training scenarios and associated controllers. Consequently, these findings highlight the importance to utilize a large and diverse scenario set to assess controller performance under process uncertainties.

4.3. State feedback controller design: Improved results

The kinetic scenarios in the training set sever as the particles' initial position in the PSO algorithm. The controllers derived from the training set Γ provide the initial design and are further improved by PSO. We execute Algorithm 1 to explore different kinetic parameters and solve associated $(\mathcal{FC})$. Table 5 shows that using a smaller kinetic value (−30%, scenario 1) in $(\mathcal{FC})$ leads to higher process efficiency than using a larger kinetic value (30%, scenario 5). This observation motivates us to slightly extend the searching range from $[0.7\tilde{\boldsymbol{k}}_0, 1.3\tilde{\boldsymbol{k}}_0]$ to $[0.69\tilde{\boldsymbol{k}}_0, 1.3\tilde{\boldsymbol{k}}_0]$ in PSO. Let particles to evolve for 16 iterations, namely $G = 16$. In Fig. 3, we plot the fitness value (process efficiency) of each particle, including the initial fitness value and 16 iterations. The D_p searching range is initially set as $D_p \in [36, 45]$. After 6 iterations, we feed all investigated kinetic samples with their optimal D_p into the MATLAB Regression Learner App to compare different regression methods. Finally, the best model, Gaussian Process Regression with Matérn kernel, is chosen for predicting D_p. This regression model achieves a root mean square error (RMSE) of 0.64 and an R^2 value of 0.91. The predicted and true optimal D_p for the initial 6 iterations are compared in Fig. 4.

During the first 6 iterations of the PSO algorithm, the best fitness value is found in 5th iteration of 5th particle. After building the optimal D_p prediction model, the PSO continues for another 10 iterations to generate a better solution found in 15th iteration of 1st particle. The **gBest** vectors obtained after the initial 6 and complete 16 iterations are shown in Table 6. In fact, the solution found in 5th iteration is also the second best controller generated by the PSO. After more iterations, the solution performance is slightly improved.

In the next step, controllers identified by the PSO are selected for the adaptive control scheme. To achieve this, a much larger kinetic set Φ, comprising 800 scenarios, is generated to represent a broader range of uncertainty. These kinetic vectors are divided into 10 clusters by using k-means approach, whose centers and number of contained scenarios are presented in Table 7. For each cluster, we use Eq. (29) to select its optimal controller from the pool. We expect that kinetic scenarios within the same cluster exhibit similar reaction rate, and thereby prefer the same controller. The average performance of each cluster, using controllers optimized by PSO, is summarized in Table 7, revealing a significant variance among clusters.

4.4. Comparison on the testing set

In this subsection, we compare the performance of benchmark MPC with the proposed state feedback controller. The kinetic parameters for both schemes are estimated through MHE with window length $D_m = 8$. It is worthwhile to note that the proposed state feedback controller only needs to locate the cluster of kinetic parameter belongs to and uses Eq. (17) to determine control actions, which normally takes 0.002 s. The MPC usually spends 35 to 85 s at each time step for online optimization during the initial reaction, which actually is longer than the sampling time $\delta = 30$ s. Therefore, the state feedback controller can at least reduce 99.994% of the online computational demand compared with MPC. We are more concerned with the average process efficiency using different control strategies. Thus, a testing set is generated, consisting of 40 independent kinetic scenarios. We tune the weighting parameters of MPC and compare it with the proposed state feedback controllers on the testing set. The results are listed in Table 8.

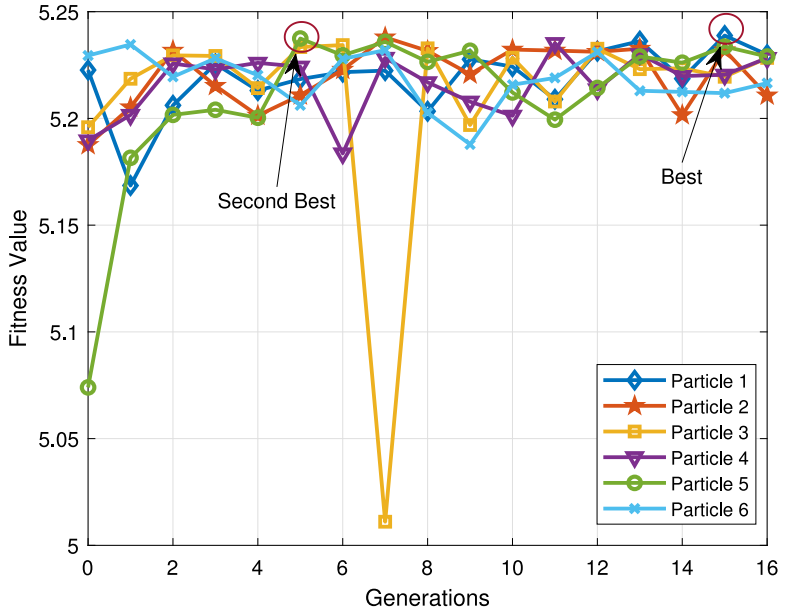

Fig. 3. The particle fitness value evolution.

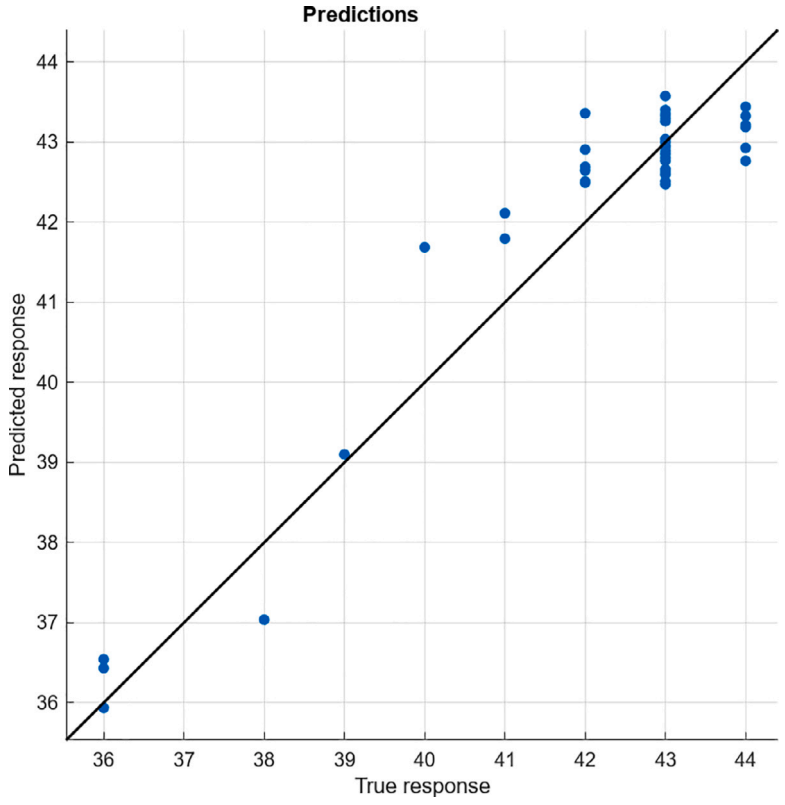

Fig. 4. The regression model performance for D_p on validation data points.

Table 6
Best kinetic parameters for ($\mathcal{FC}$) found by PSO and associated average efficiency in Π.

	$k_{0,1}$	$k_{0,2}$	$k_{0,3}$	$k_{0,4}$	$k_{0,5}$	$k_{0,6}$	$\tilde{\mathcal{E}}$
gBest after 6 iterations	0.3727	0.8071	3.4170	2.5865	0.0221	0.0284	5.2374
gBest after 16 iterations	0.3727	0.7867	3.4020	2.5870	0.0219	0.0280	5.2388

Table 7
Clusters' centers, number of scenarios, and $\tilde{\mathcal{E}}^*_{\Phi_j}$: average efficiency in Φ_j.

	$k_{0,1}$	$k_{0,2}$	$k_{0,3}$	$k_{0,4}$	$k_{0,5}$	$k_{0,6}$	Number of scenarios	$\tilde{\mathcal{E}}^*_{\Phi_j}$ after 6 iterations	$\tilde{\mathcal{E}}^*_{\Phi_j}$ after 16 iterations
Φ_1	0.6050	1.2643	3.6880	4.3847	0.0357	0.0411	94	5.2765	5.2779
Φ_2	0.6310	1.0251	3.6287	3.2180	0.0286	0.0423	71	5.3333	5.3407
Φ_3	0.4421	0.9165	4.5408	4.0078	0.0305	0.0462	81	4.7427	4.7427
Φ_4	0.5104	0.9252	4.5837	4.4195	0.0288	0.0315	69	5.0059	5.0073
Φ_5	0.4528	1.3068	4.8993	4.1615	0.0365	0.0413	69	4.8067	4.8067
Φ_6	0.6355	1.1516	5.0277	4.0835	0.0283	0.0437	75	5.4030	5.4081
Φ_7	0.4903	1.2644	4.8012	3.0347	0.0276	0.0392	89	4.9159	4.9174
Φ_8	0.6148	1.0323	5.1120	3.4425	0.0375	0.0410	90	5.4329	5.4342
Φ_9	0.4894	1.2315	3.6357	4.0439	0.0267	0.0338	66	4.8564	4.8564
Φ_{10}	0.4889	1.0493	3.6000	3.1590	0.0375	0.0359	96	4.9132	4.9132

Table 8
Comparing average process efficiency by using different control strategies.

Methods	Parameters	Average process efficiency (40 testing scenarios)
MPC1	$W_{u1} = 0$	5.0034
MPC2	$W_{u1} = 0.00005$	4.9905
State Feedback (After 6 iterations, single)	N/A	5.1464
State Feedback (After 6 iterations, adaptive)	N/A	5.1604
State Feedback (After 16 iterations, single)	N/A	5.1478
State Feedback (After 16 iterations, adaptive)	N/A	5.1616

Several discussions of these comparison results are in order:

First, we set the weighting parameter W_{u2} to zero in the MPC because electricity cost is substantially lower than the cost of methanol. Increasing W_{u1} reduces the process efficiency because it lowers methanol flow, which in turn increases the batch time.

Second, Figs. 5 and 6 depict the estimated kinetic parameters for one of the testing scenarios. In this scenario, the MPC achieves an efficiency of 5.5605, while our state feedback controller achieves an efficiency of 5.6603. Under different control strategies, the estimated $\boldsymbol{k}_0$ can be distinct due to various control actions and process outputs. The MHE requires D_m time steps for process data collection, and the estimates for some kinetic parameters diverge from their actual values due to the challenges posed by solving a high-dimensional nonlinear optimization problem. We aim to demonstrate that MPC can be very sensitive to the estimation error, whereas our state feedback control is not. During the offline design stage, we determine a suitable state feedback controller for the entire cluster that already takes uncertainty into account. This is why the state feedback controller, despite using less accurate kinetic parameters than the MPC, still shows better economic performance.

Third, the proposed state feedback controller achieves higher process efficiency than MPC on average. The kinetic uncertainty degrades the MPC's online optimization performance during the semi-batch process. In addition, since batch time is uncertain due to kinetic variability, MPC cannot directly optimize the process efficiency within its objective function. Although the proposed state feedback controller has fixed structure and relies on offline optimization, it is selected via the evaluation and clustering on numerous kinetic scenarios, making it more robust than the MPC. Direct comparisons between MPC1 ($W_{u1} = 0$) and adaptive state feedback control (after 16 iterations) are shown in Figs. 7–9. In Fig. 7, we can see that both control schemes drive the FAME concentration to the desired 98.8% across various testing scenarios, because high methanol flow ensures high yield of FAME and less batch time. However, the input signals in Fig. 8 demonstrate that state feedback controller is more aggressive due to the incorporation of target constraint (22) into the optimization formula whereas MPC ensures FAME specification through the objective function. In fact, the methanol consumption and batch time are two key factors in determining the efficiency. We can see that MPC uses less methanol F than the proposed state feedback controller. However, the proposed controller leads to a shorter batch time (39 vs 41), achieving a better trade-off between methanol consumption and batch time. Fig. 9 plots the efficiency histograms with MPC and state feedback control, respectively. Notably, the state feedback controller can regulate the process with better efficiency than the MPC in most of scenarios. Even though this improvement is only $0.16/5 = 3\%$, it yields \$0.16 more profit per 30 s. Over a year of continuous operation, this results in an annual profit increase of $0.16 \times 120 \times 24 \times 365 = \$168,192$ for the studied pilot-scale reactor. In addition, the process efficiency actually is influenced by the prices of methanol (inflow) and biodiesel (outflow). Therefore, the improvement value could be even higher if methanol or biodiesel price increases.

Fourth, we can compare the single state feedback controller and the adaptive scheme in Table 8. Efficiency results indicate that properly varying the controller according to the estimated kinetic cluster further enhances process efficiency. This clustering-based approach, which selects controllers offline designed for specific kinetic scenarios, reduces the adverse effects of estimation errors compared to directly using the estimated kinetic parameter value in online optimization.

5. Conclusion

This paper presents a novel control approach to optimize the efficiency of the biodiesel production process, specifically under conditions of kinetic uncertainty, while ensuring product quality. The proposed adaptive state feedback control scheme is implemented in two phases: an offline design phase and an online implementation phase. In the offline design phase, the uncertain kinetic parameter is sampled to generate a training set, an evaluation set, and a clustering set. State feedback controllers are designed for each scenario in the training set and their performance is evaluated using the scenarios in the evaluation set. The particle swarm optimization (PSO) and a batch time regression model are employed to further improve the controller pool. The uncertainty space is then divided into several groups based on the clustering set. Each cluster is equipped with the best-performing controller from the pool. In the online implementation phase, the moving horizon estimation (MHE) is used to estimate the kinetic parameter in real-time. Based on the estimated kinetic value, the appropriate cluster and its associated state feedback controller are selected to regulate the plant. Simulation studies, involving 40 testing scenarios, demonstrate that the proposed adaptive state feedback control approach outperforms the model predictive control (MPC) method. The designed state

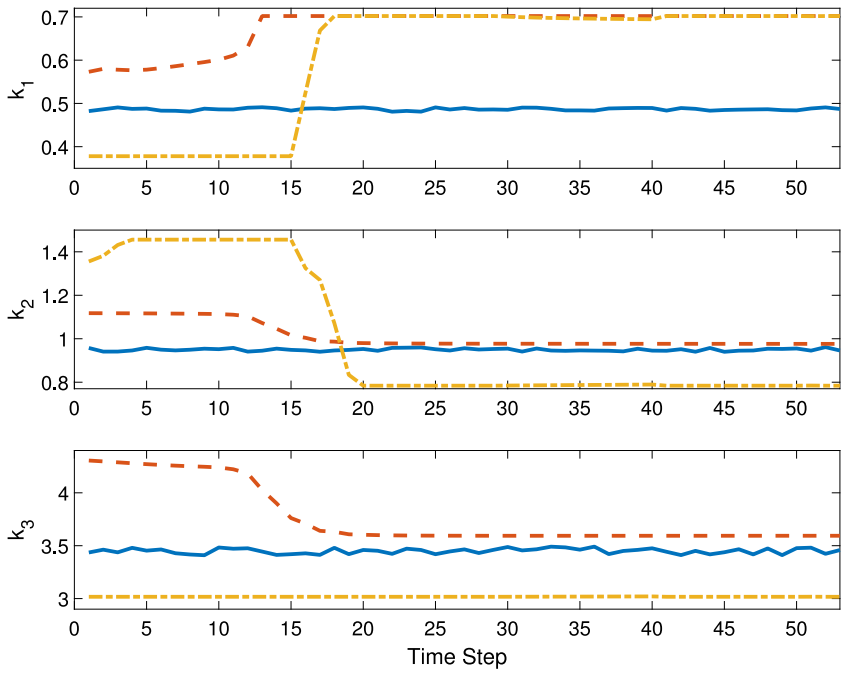

Fig. 5. The estimated value of kinetic parameters $k_1 - k_3$. Blue: Actual value; Red dash: MPC1; Yellow dash–dot: State Feedback.

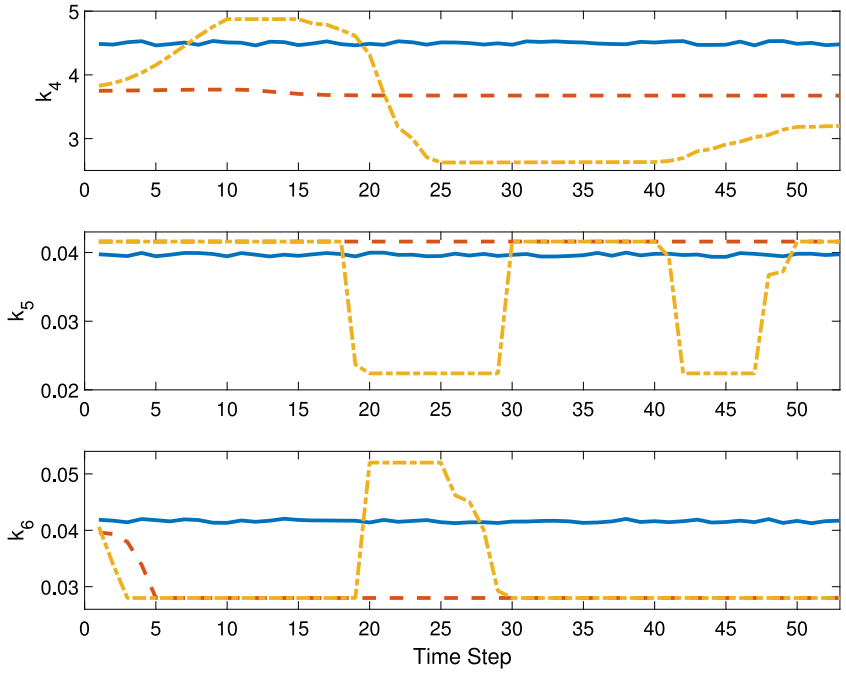

Fig. 6. The estimated value of kinetic parameters $k_4 - k_6$. Blue: Actual value; Red dash: MPC1; Yellow dash–dot: State Feedback.

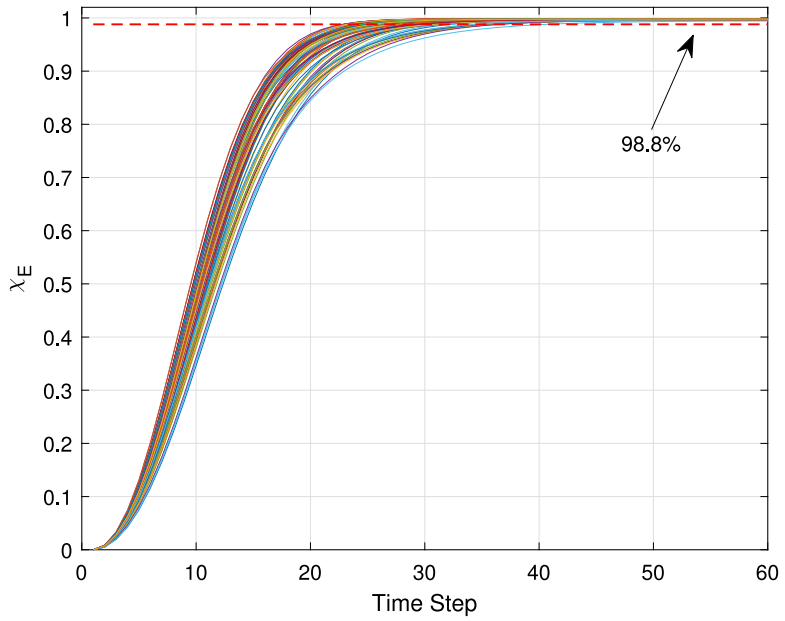

Fig. 7. The FAME percentage χ_E of the process regulated by MPC and state feedback controller. The FAME of all 40 testing scenarios finally can exceed the desired standard value 98.8% using either MPC or state feedback controller..

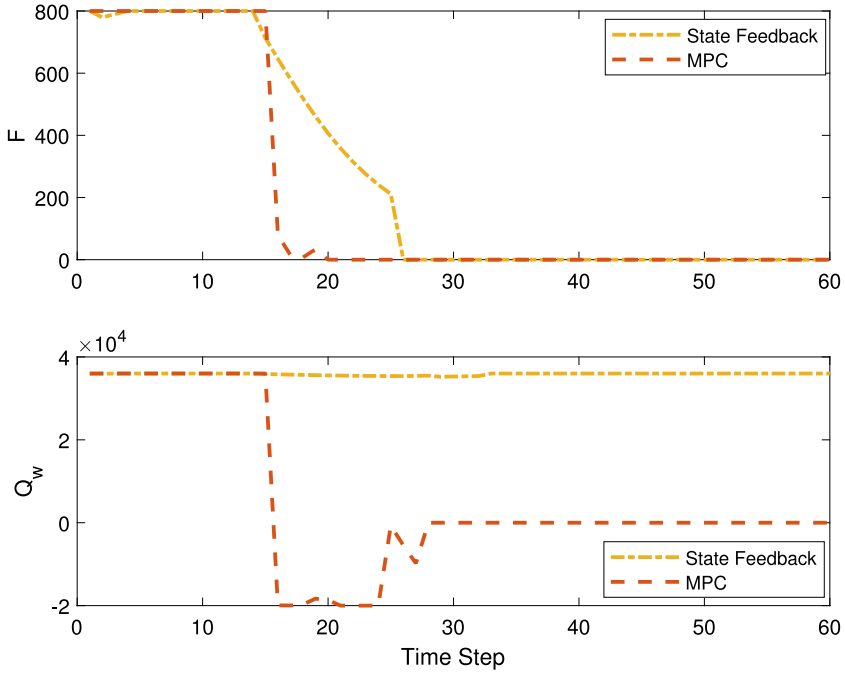

Fig. 8. The F and Q_w computed by MPC or state feedback controller in one of the testing scenarios. Batch time: MPC (41) vs. State Feedback (39).

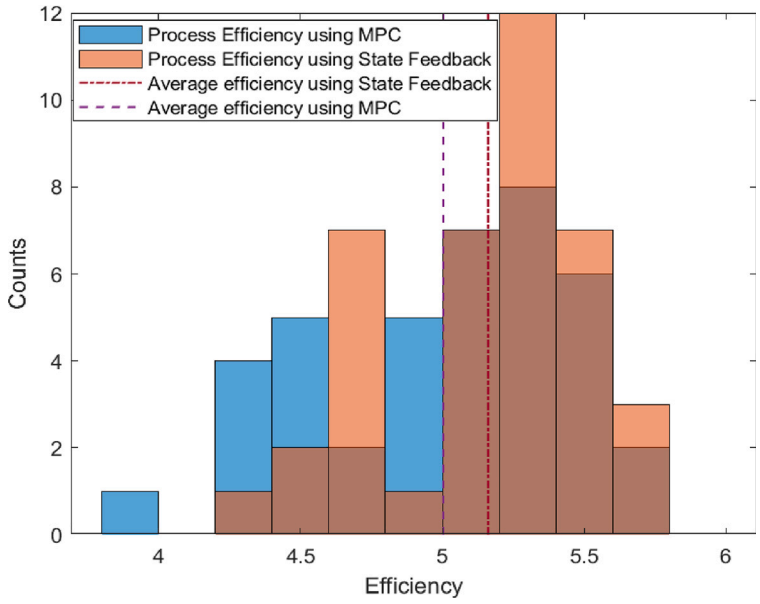

Fig. 9. The histograms of process efficiency using MPC or state feedback controller in testing scenarios.

feedback controller, enables fast calculation, achieves higher process efficiency, and exhibits greater robustness against parameter estimation errors compared to MPC. This robust performance is attributed to the extensive offline optimization and the adaptive controller selection mechanism, which effectively addresses kinetic uncertainties.

CRediT authorship contribution statement

Yu Yang: Writing – review & editing, Writing – original draft, Supervision, Software, Methodology, Investigation, Funding acquisition, Formal analysis, Data curation, Conceptualization. **Juliette Harper:** Software, Methodology, Formal analysis, Data curation, Conceptualization.

Declaration of competing interest

The authors declare that they have no known competing financial interests or personal relationships that could have appeared to influence the work reported in this paper.

Acknowledgments

The author is grateful to the financial support from National Science Foundation (NSF), United States, award number: 2151497.

References

Adloor, S.D., Vassiliadis, V.S., 2021. An optimal control approach to considering uncertainties in kinetic parameters in the maintenance scheduling and production of a process using decaying catalysts. Comput. Chem. Eng. 149, 107277.
Al-Matouq, A.A., Vincent, T.L., 2015. Multiple window moving horizon estimation. Automatica 53, 264–274.
Alessio, A., Bemporad, A., 2009. A survey on explicit model predictive control. In: Nonlinear Model Predictive Control: Towards New Challenging Applications. pp. 345–369.
Alexander, R., Dinh, S., Schultz, G., Ribeiro, M.P.A., Lima, F.V., 2023. State and covariance estimation of a semi-batch reactor for bioprocess applications. Comput. Chem. Eng. 172, 108180.
Bae, J., Kim, Y., Lee, J.M., 2021. Multirate moving horizon estimation combined with parameter subset selection. Comput. Chem. Eng. 147, 107253.
Benavides, P.T., Diwekar, U., 2012a. Optimal control of biodiesel production in a batch reactor Part I: Deterministic control. Fuel 94, 211–217.
Benavides, P.T., Diwekar, Urmila., 2012b. Optimal control of biodiesel production in a batch reactor Part II: Stochastic control. Fuel 94, 218–226.
Berchmans, H.J., Morishita, K., Takarada, T., 2010. Kinetic study of methanolysis of Jatropha curcas-waste food oil mixture. J. Chem. Eng. Jpn. 43, 661–670.
Bernardini, D., Bemporad, A., 2009. Scenario-based model predictive control of stochastic constrained linear systems. In: Proceedings of 48th IEEE Conference on Decision and Control. pp. 6333–6338.
Brásio, S.R., Romanenko, A., Leal, J., Santos, L.O., Fernandes, N., 2013. Nonlinear model predictive control of biodiesel production via transesterification of used vegetable oils. J. Process Control 22, 1471–1479.
Dong, Z., Angeli, D., 2020. Homothetic tube-based robust economic MPC with integrated moving horizon estimation. IEEE Trans. Automat. Control 66, 64–75.
Ellis, M., Durand, H., Christofides, P.D., 2014. A tutorial review of economic model predictive control methods. J. Process Control 24, 1156–1178.
Engell, S., 2007. Feedback control for optimal process operation. J. Process Control 17, 203–219.
Graboski, M.S., McCormick, R.L., 1998. Combustion of fat and vegetable oil derived fuels in diesel engines. Prog. Energy Combust. Sci. 24, 125–164.
Haseltine, E.L., Rawlings, J.B., 2005. Critical evaluation of extended Kalman filtering and moving-horizon estimation. Ind. Eng. Chem. Res. 44, 2451–2460.
Huang, R., Patwardhan, S.C., Biegler, L.T., 2012. Robust stability of nonlinear model predictive control based on extended Kalman filter. J. Process Control 22, 82–89.
Jung, T.Y., Nie, Y., Lee, J.H., Biegler, L.T., 2015. Model-based on-line optimization framework for semi-batch polymerization reactors. IFAC-PapersOnLine 48, 164–169.
Kummer, A., Nagy, L., Varga, T., 2020. NMPC-based control scheme for a semi-batch reactor under parameter uncertainty. Comput. Chem. Eng. 141, 106998.
Kwon, J.S., Nayhouse, M., Orkoulas, G., Ni, D., Christofides, P.D., 2015. A method for handling batch-to-batch parametric drift using moving horizon estimation: Application to run-to-run MPC of batch crystallization. Chem. Eng. Sci. 127, 210–219.
Lee, J.H., Lee, K.S., 2007. Iterative learning control applied to batch processes: An overview. Control Eng. Pract. 15, 1306–1318.
Limon, D., Alvarado, I., Alamo, T., Camacho, E.F., Robust tube-based MPC for tracking of constrained linear systems with additive disturbances. J. Process Control 20, 248–260, 210.
Lucia, S., Andersson, J., Brandt, H., Diehl, M., Engell, S., 2014. Handling uncertainty in economic nonlinear model predictive control: A comparative case study. J. Process Control 24, 1247–1259.
Mayne, D.Q., Seron, M.M., Raković, S.V., 2005. Robust model predictive control of constrained linear systems with bounded disturbances. Automatica 41, 219–224.
Mhaskar, P., El-Farra, N.H., Christofides, P.D., 2006. Stabilization of nonlinear systems with state and control constraints using Lyapunov-based predictive control. Systems Control Lett. 55, 650–659.
Montagner, V.F., Leite, V.J.S., Oliveira, R.C.L.F., Peres, P.L.D., 2006. State feedback control of switched linear systems: An LMI approach. J. Comput. Appl. Math. 194, 192–206.
Nagy, Z.K., Braatz, R.D., 2003. Robust nonlinear model predictive control of batch processes. AIChE J. 49, 1776–1786.
Narendra, K., Balakrishnan, J., 1997. Adaptive control using multiple models. IEEE Trans. Autom. Control 42, 171–187.
Rao, C.V., Rawlings, J.B., Lee, J.H., 2001. Constrained linear state estimation-a moving horizon approach. Automatica 37, 1619–1628.

Rawlings, J.B., Angeli, D., Bates, C.N., 2012. Fundamentals of economic model predictive control. In: Proceedings of 51st IEEE Conference on Decision and Control. CDC.

Voelker, A., Kouramas, K., Pistikopoulos, E.N., 2013. Moving horizon estimation: Error dynamics and bounding error sets for robust control. Automatica 49, 943–948.

Wächter, A., Biegler, L.T., 2006. On the implementation of a primal–dual interior point filter line search algorithm for large-scale nonlinear programming. Math. Program. 106, 25–57.

Wang, F.Y., Bahri, P., Lee, P.L., Cameron, I.T., 2007. A multiple model, state feedback strategy for robust control of non-linear processes. Comput. Chem. Eng. 31, 410–418.

Wang, J., Chen, C., Zhao, F., Wang, J., Li, A., 2023. Process optimization of microbial fermentation with parameter uncertainties via distributionally robust discrete control. J. Process Control 132, 103116.

Zhan, Z.-H., Zhang, J., Li, Y., Chung, H.S-H., 2009. Adaptive particle swarm optimization. IEEE Trans. Syst. Man Cybern.-B: Cybernetics 39, 1362–1381.